FACTA UNIVERSITATIS
Series: **Architecture and Civil Engineering** Vol. 18, Nº 3, 2020, pp. 241-260
https://doi.org/10.2298/FUACE200422018Z

MATHEMATICAL INTERPRETATION OF SEISMIC WAVE SCATTERING AND REFRACTION ON TUNNEL STRUCTURES OF CIRCULAR CROSS-SECTION

UDC 550.344.094.4
517.518.45
624.19

Elefterija Zlatanović[1], Vlatko Šešov[2], Dragan Lukić[3], Zoran Bonić[1]

[1]University of Niš, Faculty of Civil Engineering and Architecture of Niš, Niš, Serbia
[2]University "Ss. Cyril and Methodius" of Skopje, Institute of Earthquake Engineering and Engineering Seismology, Skopje, North Macedonia
[3]University of Novi Sad, Faculty of Civil Engineering of Subotica, Subotica, Serbia

Abstract. *Mathematical interpretation of the elastic wave diffraction in circular cylinder coordinates is in the focus of this paper. Firstly, some of the most important properties of Bessel functions, pertinent to the elastic wave scattering problem, have been introduced. Afterwards, basic equations, upon which the method of wave function expansions is established, are given for cylindrical coordinates and for plane-wave representation. In addition, steady-state solutions for the cases of a single cavity and a single tunnel are presented, with respect to the wave scattering and refraction phenomena, considering both incident plane harmonic compressional and shear waves. The last part of the work is dealing with the translational addition theorems having an important role in the problems of diffraction of waves on a pair of circular cylinders*.

Key words: *circular tunnel, seismic waves, scattering, refraction, Fourier–Bessel series*

1. INTRODUCTION

In a boundless medium of homogeneous characteristics, seismic waves propagate without interruption, with a constant velocity and along a certain path. The presence of an inhomogeneity in the ground properties generally produces a significant influence on waves propagating through the medium.

Received April 22, 2020 / Accepted February 11, 2021
Corresponding author: Elefterija Zlatanović
University of Niš, Faculty of Civil Engineering and Architecture of Niš, Aleksandra Medvedeva 14, 18000 Niš, Serbia
E-mail: elefterija2006@yahoo.com

The wave, which emanates from infinite depth in one of the media, is called the *incident wave*. After impinging on inhomogenity (obstacle), the path of the wave propagation is changed, i.e. waves reflect and refract in indistinct patterns depending on the shape and properties of irregularity and surrounding ground. When an incident body wave, propagating through elastic medium, arrives at any discontinuity (e.g., free surface, empty cavity, crack), it will be fully returned back into the medium (*reflected waves*). This is the special case of the second medium that cannot transmit mechanical waves, like a vacuum or air, when the incident wave is completely reflected. For the case of incident seismic waves arriving at the contact surface with another elastic medium (e.g., another ground layer or tunnel lining), a part of its energy will be transmitted into the other medium (*refracted waves*), whereas the remaining energy will return back into the first medium (*reflected waves*) [1].

When excited by the undisturbed incident wave, the obstacle acts as a secondary source by emitting waves radially outward from itself. The deviation of the wave from its original path is considered to be *diffraction*, whereas the radiation of secondary waves from the obstacle is referred to as *scattering*. Diffraction and scattering result in amplification and deamplification of the incident seismic waves in the region near the obstacle, which stands for a phenomenon known as *dynamic stress concentration* [2].

The methods of studying the diffraction of elastic waves are not much different from those concerning other types of waves, owing to physical similarity and mathematical analogy. Nevertheless, there is an additional difficulty in the analysis, as the incident wave diffraction phenomenon in isotropic elastic medium is associated with the coexistence of two types of scattered waves with distinct wave propagation velocity, in contrast to one acoustical or electromagnetic wave in air. In order to understand the nature of the reflected and the refracted waves, the case of wave propagation in two-layered elastic formation is considered, as illustrated in the following figure (Fig. 1).

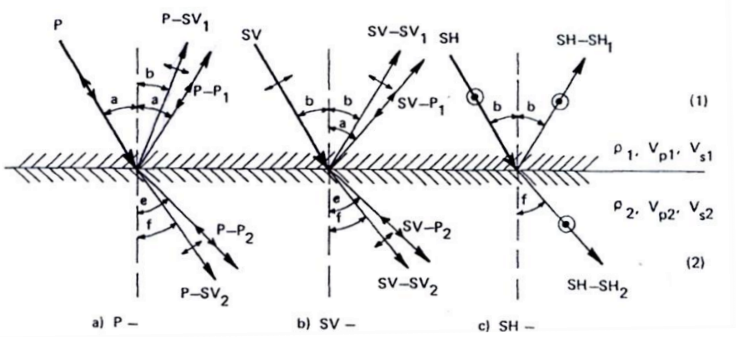

Fig. 1 Breaking down of elastic wave at the boundary between two elastic media [1]

In general, it should be anticipated that a P-wave incident on the interface of two elastic media will give rise to reflection and transmission of P-waves, but also to reflection and transmission of transverse SV-waves with the displacement polarised in vertical plane. Similarly, the vertical component of an S-wave (SV-wave) will cause the appearance of a reflected SV-wave and a P-wave, as well as a refracted SV-wave and a P-wave. The horizontal component of the S-wave (SH-wave), however, is associated with occurrence of only S-waves: a reflected SH-wave and a refracted SH-wave.

If a body has a finite cross-sectional dimension, such as a circular cylinder of infinite length, waves bounce back and forth between the bounding surfaces. Although it is very difficult to trace the actual reflections in that case, it can be observed that the general direction of energy transmission is in a direction parallel to the bounding surfaces, and it is said that the waves are propagating in a waveguide. Hence, there is a standing wave across the cross-section of the body and a travelling wave in the direction of the waveguide [3].

2. Bessel Functions and Certain of Their Properties

The subsequent brief introduction to Bessel functions and their most important characteristics for analysis of the elastic wave diffraction and scattering problem has included the works of Mow and Pao [2], Abramowitz and Stegun [4], Watson [5], and Ivanov [6].

2.1. Bessel's equation

The second-order differential equation of the form:

$$x^2 \frac{\mathrm{d}^2 y}{\mathrm{d}x^2} + x \frac{\mathrm{d}y}{\mathrm{d}x} + (x^2 - \nu^2) y = 0 \tag{1}$$

is known as *Bessel's equation of order v*. It is characterised by two singular points: the regular singular point $x = 0$ and the irregular singular point $x = \infty$.

The constant v defines the order of the Bessel functions found as the solution to the Bessel's differential equation and can take on any real-numbered value. In case of cylindrical problems, the order of the Bessel function is an integer value ($v = n$).

Considering that the Bessel's differential equation is a second-order equation, there must be two linearly independent solutions. Typically the general solution is given as:

$$y = AJ_\nu(x) + BY_\nu(x) \tag{2}$$

The functions $J_v(x)$ and $Y_v(x)$ are the solutions of Eq. (1).

The former is called the *Bessel function of the first kind of order v*, whereas the latter is called the *Bessel function of the second kind of order v* and is sometimes referred to as a Weber function or a Neumann function $N_v(x)$.

2.2. Bessel function of the first kind

The Bessel functions of the first kind of integer order $n = 0$, 1, 2, and 3 are shown in Fig. 2.

From Fig. 2 it is perceivable that J_n are oscillatory functions and, in fact, they resemble damped trigonometric functions. In particular, the behaviour of J_0 looks like a cosine curve with slight damping, whereas J_1 resembles that of the sine function. In addition, the graph illustrates the property of the Bessel function that, as n is being of a higher value, the Bessel function starts up much slower. After this initial sluggish start for larger values of n, the functions behave roughly like a sine (odd n) or cosine (even n) multiplied by a magnitude factor that decays slowly as $x \to \pm \infty$.

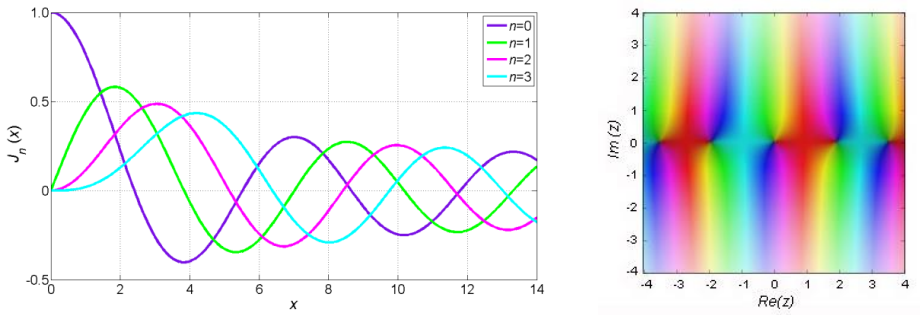

Fig. 2 Presentation of the Bessel functions of the first kind of integer orders: (left) on the real line for n = 0, 1, 2, 3; (right) in the complex plane

2.3. Bessel function of the second kind

Based on Fig. 3, it is obvious that as $x \rightarrow 0$ all $Y_n(x) \rightarrow -\infty$ due to the logarithmic singularity. Therefore, plots start a little away from 0. The functions with the higher values of n diverge to infinity ($-\infty$) more rapidly as x tends to 0. After the initial divergence, the functions settle into the familiar damped oscillation. $Y_n(x)$ is neither an even nor odd function of x.

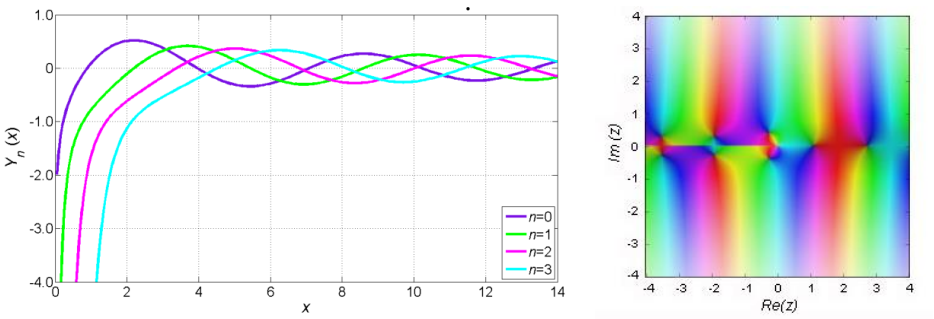

Fig.3 Presentation of the Bessel functions of the second kind of integer orders: (left) on the real line for n = 0, 1, 2, 3; (right) in the complex plane

Considering the two functions J and Y of any order, e.g. J_0 and Y_0, on the same graph (Fig. 4), it is perceptible that for larger x they resemble damped trigonometric functions differing only in a phase shift.

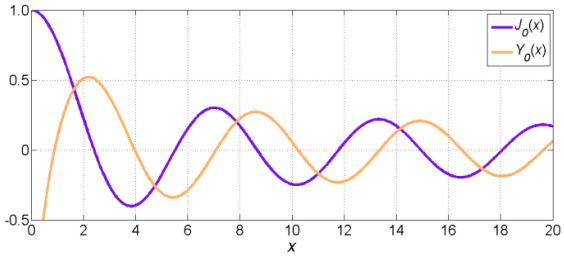

Fig. 4 Presentation of the Bessel functions of the first and second kind of order n = 0

2.4. Hankel functions of the first and second kind

The Hankel functions of order *v* represent the complex sum of the Bessel functions of the first and second kind (in which $\mathrm{i} = \sqrt{-1}$ designates the imaginary unit):

$$H_\nu^{(1)}(x) = J_\nu(x) + \mathrm{i}Y_\nu(x) \tag{3}$$

$$H_\nu^{(2)}(x) = J_\nu(x) - \mathrm{i}Y_\nu(x) \tag{4}$$

The functions $H_\nu^{(1)}(x)$ and $H_\nu^{(2)}(x)$ are called the *Hankel functions of the first* and *second kind of order v*, respectively, and are also known as the Bessel functions of the third kind. Owing to the linear independence of the Bessel function of the first and second kind, the Hankel functions provide an alternative pair of solutions to the Bessel differential equation. Both of the functions are infinite at $x = 0$ and their fruitfulness is related to their behaviour for large values of *x*, in other words, the series cannot be used for very large values of *x*. The behaviour of the Hankel functions can be introduced through the properties of *J* and *Y* (Figs. 5 and 6).

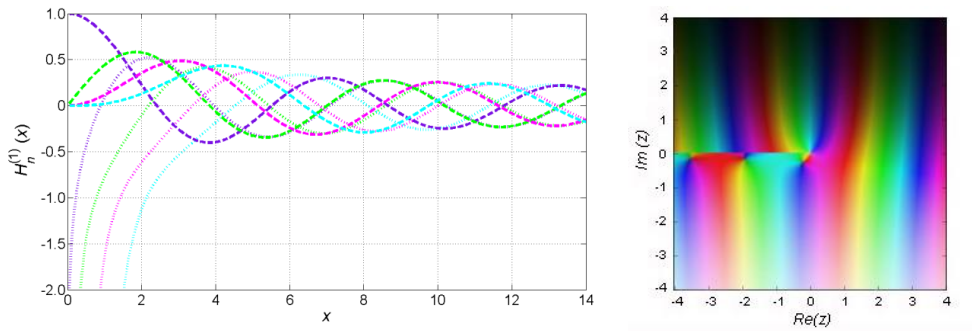

Fig. 5 Presentation of the Hankel functions of the first kind of integer orders: (left) on the real line for $n = 0, 1, 2, 3$; (right) in the complex plane

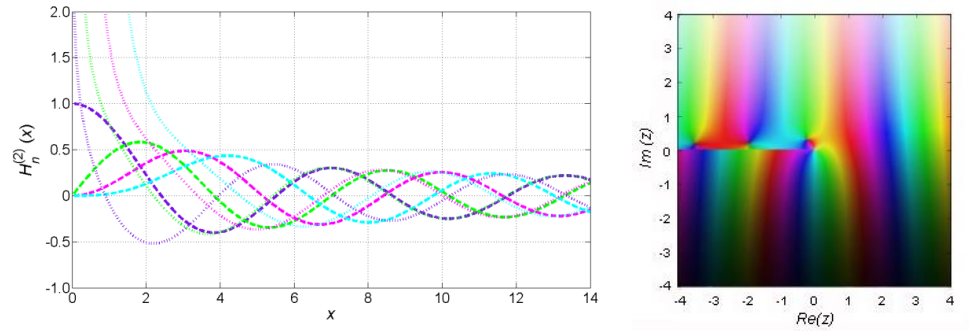

Fig. 6 Presentation of the Hankel functions of the second kind of integer orders: (left) on the real line for $n = 0, 1, 2, 3$; (right) in the complex plane

3. WAVE EQUATIONS AND SOLUTION IN CYLINDRICAL COORDINATES

In vector notation, **displacement equations of motion**, which govern the motion of a homogeneous, isotropic, linearly elastic medium of infinite extent, are a system of partial differential equations of the following form [3]:

$$(\lambda + \mu)\boldsymbol{\nabla}\boldsymbol{\nabla} \cdot \mathbf{u} + \mu\nabla^2\mathbf{u} + \rho\mathbf{f} = \rho\ddot{\mathbf{u}} \tag{5}$$

where dots over a quantity mean the partial derivative with respect to time t, ρ is the mass density, λ and μ are known as Lame's constants, $\mathbf{u}$ and $\mathbf{f}$ are displacement vector and force vector, respectively, whereas $\boldsymbol{\nabla}$ is the vector differential operator (nabla) and ∇^2 is the Laplacian, given as follows (with $\mathbf{e_1}$, $\mathbf{e_2}$, and $\mathbf{e_3}$ being the unit vectors of the coordinate axes x_i):

$$\boldsymbol{\nabla} = \frac{\partial}{\partial x_1}\mathbf{e_1} + \frac{\partial}{\partial x_2}\mathbf{e_2} + \frac{\partial}{\partial x_3}\mathbf{e_3} \tag{6}$$

$$\nabla^2 = \frac{\partial^2}{\partial {x_1}^2} + \frac{\partial^2}{\partial {x_2}^2} + \frac{\partial^2}{\partial {x_3}^2} \tag{7}$$

3.1. Displacement potentials and reduction to wave equations

The previously presented system of equations (Eq. 5) implies three displacement components. One of the possibilities the system to be uncoupled is to express the components of the displacement vector in terms of derivatives of potentials.

By applying the *Helmholtz decomposition theorem* [3], the displacement fields can be represented as superposition of longitudinal and transverse vector components. This procedure is known as the *Helmholtz decomposition of a vector*, and it states that any vector field can be expressed as the sum of the gradient of a scalar field φ and the curl of a vector field $\boldsymbol{\psi}$:

$$\mathbf{u} = \boldsymbol{\nabla}\varphi + \boldsymbol{\nabla} \times \boldsymbol{\psi} \tag{8}$$

where φ stands for the *scalar displacement potential* and $\boldsymbol{\psi}$ represents the *vector displacement potential*. Substituting the displacement representation (Eq. 8) into Eq. (5) and considering that $\boldsymbol{\nabla} \cdot \boldsymbol{\nabla}\varphi = \nabla^2\varphi$ and $\boldsymbol{\nabla} \cdot \boldsymbol{\nabla} \times \boldsymbol{\psi} = 0$, the equation of motion (when body forces are neglected) can be rewritten as:

$$\boldsymbol{\nabla}[(\lambda + 2\mu)\nabla^2\varphi - \rho\ddot{\varphi}] + \boldsymbol{\nabla} \times \left[\mu\nabla^2\boldsymbol{\psi} - \rho\ddot{\boldsymbol{\psi}}\right] = 0 \tag{9}$$

and it is clearly satisfied if:

$$c_P^2\nabla^2\varphi = \ddot{\varphi} \tag{10}$$

$$c_S^2\nabla^2\boldsymbol{\psi} = \ddot{\boldsymbol{\psi}} \tag{11}$$

where c_P and c_S are the corresponding wave propagation velocities in the elastic medium:

$$c_P = \sqrt{\frac{\lambda + 2\mu}{\rho}} \tag{12}$$

$$c_S = \sqrt{\frac{\mu}{\rho}} \tag{13}$$

The wave arising from $\nabla\varphi$ is the primary wave (P-wave) with propagation velocity c_P, whereas the one from $\nabla \times \boldsymbol{\psi}$ is the secondary wave (S-wave) with propagation velocity c_S. The displacement potentials φ and $\boldsymbol{\psi}$ satisfy a scalar and a vector wave equation, respectively. Equations (10) and (11) are uncoupled wave equations.

Since $\boldsymbol{\psi}$ gives rise to a shear wave, the resolution of a plane shear wave into SV-wave and SH-wave (Fig. 7) suggests that $\boldsymbol{\psi}$ may be decomposed into two parts. The first part is a vector along a preferred direction, usually one of the coordinate axes, e.g. $\mathbf{e_3}$, and the other one is perpendicular to the first vector, i.e. in the x_1Ox_2-plane. Consequently, the following expression arises:

$$\boldsymbol{\psi} = \psi\mathbf{e_3} + \nabla \times (\chi\mathbf{e_3}) \tag{14}$$

where ψ and χ are two scalar functions.

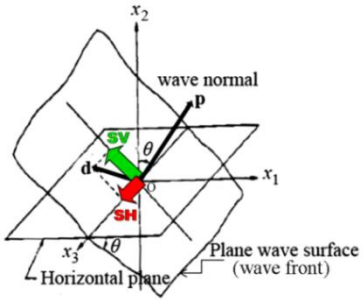

Fig. 7 Polarisation of S-wave

Taking into consideration the Helmholtz decomposition theorem for representation of the displacement fields as the superposition of longitudinal and transverse vector components, the displacements are obtained in the following form:

$$\mathbf{u} = \nabla\varphi + \nabla \times (\psi\mathbf{e_3}) + \nabla \times \nabla \times (\chi\mathbf{e_3}) \tag{15}$$

in which the second member $\nabla \times (\psi\mathbf{e_3}) = \nabla(\psi) \times \mathbf{e_3}$ is perpendicular to the unit vector $\mathbf{e_3}$, whereas the third component is defined by the unit vector $\mathbf{e_3}$. If $\mathbf{e_3}$ is taken along the wave normal, ψ and χ give rise to the plane SV- and SH-wave, respectively. Scalar potentials φ, ψ, and χ satisfy the following scalar wave equations:

$$\begin{aligned} c_P^2\nabla^2\varphi &= \ddot{\varphi} \\ c_S^2\nabla^2\psi &= \ddot{\psi} \\ c_S^2\nabla^2\chi &= \ddot{\chi} \end{aligned} \tag{16}$$

The wave equations reduce to the familiar Helmholtz equation for steady-state response [3]. Steady-state solutions are considered to be of the following form:

$$\varphi(x_i, t) = \phi(x_i, \omega)\, \mathrm{e}^{-\mathrm{i}\omega t} \tag{17}$$

where x_i are coordinates of the position vector **x**.

If a steady-state solution of the form given in Eq. (17) is substituted into the wave equation with inhomogeneous terms:

$$\nabla^2\varphi(x_i,t) - \frac{1}{c^2}\ddot{\varphi}(x_i,t) = -F(x_i,\omega)\,\mathrm{e}^{-\mathrm{i}\omega t} \tag{18}$$

the following equation is introduced:

$$\nabla^2\phi(x_i,\omega) + k^2\phi(x_i,\omega) = -F(x_i,\omega) \tag{19}$$

where $k = \omega/c$ is the so-called wavenumber, which represents the number of wavelengths L over 2π ($k = 2\pi/L$), ω is circular frequency $\omega = 2\pi f$ (radians per unit time) with f being the frequency (in Hz), and c is the wave propagation velocity.

The homogeneous form of Eq. (19) is called the space form of the wave equation, which is known as *Helmholtz equation.*

3.2. Solutions to the Helmholtz equation in cylindrical coordinates

If the function φ is of the form $\varphi(r,\theta,z,t) = \phi(r,\theta,z,\omega)\,\mathrm{e}^{-\mathrm{i}\omega t}$, it must satisfy the Helmholtz scalar wave equation (the homogeneous form of Eq. (19)) that in the system of cylindrical coordinates (r, θ, z) has the following form:

$$\nabla^2\phi(r,\theta,z,\omega) + k^2\phi(r,\theta,z,\omega) = 0 \tag{20}$$

in which case the Laplacian is defined as:

$$\nabla^2 = \frac{\partial^2}{\partial r^2} + \frac{1}{r}\frac{\partial}{\partial r} + \frac{1}{r^2}\frac{\partial^2}{\partial\theta^2} + \frac{\partial^2}{\partial z^2} \tag{21}$$

The corresponding wave functions are usually derived by separating the variables in the wave equations (*method of separation of variables* [2]). If the particular solution to Eq. (20) is sought in the form of the product of three functions:

$$\phi(r,\theta,z) = R(r)\,\Theta(\theta)\,Z(z) \neq 0 \tag{22}$$

where each of these functions depends only on one coordinate, then the Helmholtz equation can be separated into three ordinary differential equations, one for each coordinate at the time:

$$r^2R'' + rR' + (k^2r^2 - \nu^2)R = 0 \tag{23}$$

$$\Theta'' + \nu^2\Theta = 0 \tag{24}$$

$$Z'' + \gamma^2 Z = 0 \tag{25}$$

in which ν and γ are separation constants.

The equation with the variable r is the *radial function*, whereas the other two are *angular functions*. Therefore, the product of the radial and angular functions constitutes the cylindrical wave functions. The solutions for Θ and Z are:

$$\Theta = \mathrm{e}^{\pm\mathrm{i}\nu\theta} \tag{26}$$

$$Z = \mathrm{e}^{\pm\mathrm{i}\gamma z} \tag{27}$$

The solutions of the equation for $\Theta(\theta)$ are sines and cosines of the argument $v\theta$. For most problems of interest, Θ must be single valued, i.e. $\Theta(\theta + 2\pi) = \Theta(\theta)$, in which case v can only be zero or an integer n. In addition, the solutions should be continuous functions of θ, with continuous derivatives, thus requiring $v = n$.

The equation Eq. (22) is the Bessel ordinary differential equation, and accordingly, its solutions are Bessel functions. The solution to $R(r)$, when $v = n$, can be expressed in terms of either the Bessel functions of the first and second kind, $J_n(kr)$ and $Y_n(kr)$, or the Hankel functions of the first and second kind, $H_n^{(1),\,(2)}(kr)$. The choice of the radial function is dependent upon the physics of the problem.

As it has been discussed in Section 2.2, the function $J_n(x)$ is regular at the point $x = 0$. Therefore, this function is ordinarily used for constructing a general solution to Eq. (20) inside the cylindrical region containing within itself $r = 0$, thus representing the waves that propagate towards the interior of the cylinders.

On the other hand, functions $H_n^{(1),(2)}(x)$, when are combined with the time factor $e^{-i\omega t}$, represent cylindrical waves generated by a source on an obstacle. At the point $x = 0$, these functions have a logarithmic singularity. The function $H_n^{(1)}(kr)\, e^{-i\omega t}$ represents a diverging or outgoing cylindrical wave; that is, the waves as generated by a circular barrier propagating away from its centre. Similarly, the function $H_n^{(2)}(kr)\, e^{-i\omega t}$ represents a converging or incoming cylindrical wave. The boundary condition at $r = \infty$ in this problem eliminates the latter from the scattered waves. Namely, the scattered waves should satisfy the equations of motion and at infinity, in the unbounded region outside the cylinder, the condition of radiation (the Sommerfeld radiation conditions [3]), and by that, these functions represent outgoing waves that emanate from the origin of the circular cylinder. Therefore, only the function with $H_n^{(1)}(kr)$ can be used in a definition of the scattered wave field.

Accordingly, the particular solutions to the Helmholtz equation (Eq. (20)) will be the following functions:

$$J_n(kr)\, e^{in\theta} e^{i\gamma z} \tag{28}$$

$$H_n^{(1)}(kr)\, e^{in\theta} e^{i\gamma z} \tag{29}$$

The separation constants γ and k may be referred to as propagation constants in z and r directions, respectively, although they are related by Eq. (20) as $k^2 = \omega^2/c^2 - \gamma^2$, and are to be determined from the corresponding boundary conditions of the problem. Thus, for example, if a wave is propagating in the xOy-plane, then ϕ will be independent of z and $\gamma = 0$. It follows that $k = \omega/c$, which is the common definition of the wavenumber. Generally, the separation constant γ could be complex. Therefore, the field is not necessarily periodic along the z-axis.

Bessel's equation, given by Eq. (1) at the beginning, is applicable in those cases when the solution is oscillatory in r and exponential in z. In other problems, the homogeneous boundary conditions are on the surfaces of constant z, making the solutions oscillatory in z. In those cases, the separation constant has a sign opposite to that in the presented Bessel's equation, and the resulting radial displacement is the *modified Bessel equation*, in which case the solution are the modified Bessel functions of the first and second kind, $I_n(kr)$ and $K_n(kr)$, respectively.

4. WAVE FUNCTIONS EXPANSION METHOD

The essence of the method of wave functions expansion is in expressing the corresponding waves in terms of a series of wave functions [2]. In finding the solution of diffraction problems by this method, the diffracting body is usually represented in the form of a sum of a known primary field and an unknown secondary field scattered on barriers. The field inside the scattering body is taken in the form of an infinite series of primary wave functions, not having singularities in the volume of the body, whereas the field outside is superposed in the form of an infinite series of primary wave functions that satisfy the condition of radiation at infinity. The unknown coefficients in the series expansion are determined from the magnitude of the incident waves and the appropriate boundary conditions.

This method has gained importance and is widely used due to the rapid convergence of the series solution. The fast convergence of the series solution is achieved in particular for the case of low-frequency waves with long wavelengths (i.e., small wavenumber k), and in the neighborhood of the obstacle (i.e., small x), whereas for the case of much shorter incident wavelengths (high frequencies), or for greater distances from the obstacle, the series solution converges considerably slower.

Nevertheless, only regular-shaped scatterers, such as circular, elliptical, and parabolic cylinders, spheres, etc., are suitable for this method. For problems approximated by plane strain and anti-plane strain, this method is applicable to scatterers of circular, elliptical, or parabolic cross-section, because the obstacle must be of the shape of a long cylinder.

As circular-cylinder-shaped scatterers are in the focus of this study, for this concern, in the subsequent part the general solutions for wave equations in circular cylinder coordinates will be presented, considering the steady-state time-harmonic waves. Having in mind that the transient solution is usually determined based on the steady-state solution, accordingly, no generality is lost in the presentation.

5. STEADY-STATE SOLUTION FOR A CAVITY AND A TUNNEL UNDER INCIDENT PLANE HARMONIC WAVES

For the purpose of the following presentation of the steady-state solution concerned with incident plane harmonic waves, an obstacle (cavity/tunnel) is assumed to be a long, uniform cylinder with a circular cross-section in a boundless medium, which is referred to a coordinate system as shown in Fig. 8. It is common to take the axis of the cylinder along the z-direction, and the wave normal $\mathbf{p}$ of a plane wave, in general case, to be inclined to the z-axis (oblique incidence).

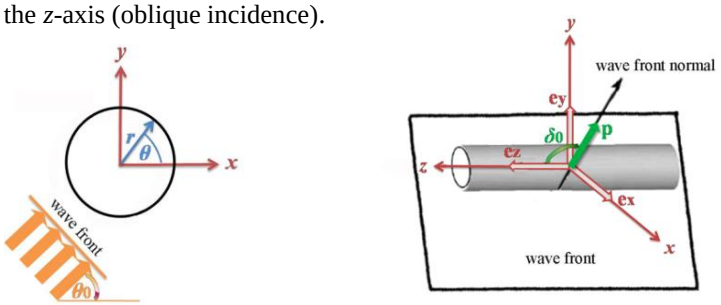

Fig. 8 Plane wave geometry

According to Fig. 8, the unit vector **p** makes an angle δ_0 with the *z*-axis (out-of-plane incidence angle) and its projection in the *x*O*y*-plane is at an angle θ_0 relative to the *x*-axis (in-plane incidence angle), i.e. θ_0 is the angle that the normal of intersection between the *x*O*y*-plane and the wave front makes with the *x*-axis. Accordingly, for $\theta_0 = 0$ the incident seismic waves will be parallel to *x*O*z*-plane, whereas for $\theta_0 = \pi/2$ the incident waves are parallel to *y*O*z*-plane. On the other hand, for $\delta_0 = \pi/2$ the plane-strain conditions are valid. In case when the propagation vector is at an arbitrary angle with the longitudinal cylinder axis, a full three-dimensional treatment of the problem is required. Yet, the solution can be formulated in a manner for which the plane-strain approximation can be applied.

5.1. Expansion of incident plane waves for cylindrical wave functions

5.1.1. Incident plane harmonic P-wave in cylindrical coordinates

The incident plane P-wave in polar coordinates, in general case, is represented by infinite Fourier–Bessel series [2, 3]:

$$\varphi^{inc}(r,\theta,z,t) = \varphi_0 \, \mathrm{e}^{\mathrm{i}k_p z \cos\delta_P} \, \mathrm{e}^{-\mathrm{i}\omega t} \sum_{n=-\infty}^{\infty} \mathrm{i}^n J_n(k_P r \sin\delta_P) \, \mathrm{e}^{\mathrm{i}n(\theta-\theta_0)} \tag{30}$$

For the potential φ^{inc} in Eq. (30), the *z*-dependence is separated from the remaining space and time variables. By introducing the relations $\alpha = k_P \sin\delta_P$ and $\gamma_P = k_P \cos\delta_P$, the expansion of the plane P-wave for the cylindrical wave functions is found to be:

$$\varphi^{inc}(r,\theta,z,t) = \varphi_0 \, \mathrm{e}^{\mathrm{i}(\gamma_p z-\omega t)} \sum_{n=-\infty}^{\infty} \mathrm{i}^n J_n(\alpha r) \, \mathrm{e}^{\mathrm{i}n(\theta-\theta_0)} \tag{31}$$

where α is the **compressional wavenumber** and $\alpha^2 = {k_P}^2 - {\gamma_P}^2 = \omega^2/{c_P}^2 - {\gamma_P}^2$.

In *plane-strain conditions* ($\delta_P = \pi/2$), when $\gamma_P = 0$, the compressional wavenumber will be of the form $\boldsymbol{\alpha = k_P = \omega/c_P}$ (Section 3.1).

5.1.2. Incident plane harmonic S-wave in cylindrical coordinates

Scattering due to each component of S-wave can be treated independently.

In accordance with this, the expansion of the plane S-wave for the cylindrical wave functions in terms of Fourier–Bessel series is of the following form:

$$\psi^{inc}(r,\theta,z,t) = \psi_0 \, \mathrm{e}^{\mathrm{i}(\gamma_S z-\omega t)} \sum_{n=-\infty}^{\infty} \mathrm{i}^n J_n(\beta r) \, \mathrm{e}^{\mathrm{i}n(\theta-\theta_0)} \tag{32}$$

$$\chi^{inc}(r,\theta,z,t) = \chi_0 \, \mathrm{e}^{\mathrm{i}(\gamma_S z-\omega t)} \sum_{n=-\infty}^{\infty} \mathrm{i}^n J_n(\beta r) \, \mathrm{e}^{\mathrm{i}n(\theta-\theta_0)} \tag{33}$$

in which β is the **shear wavenumber** referring to the relations $\beta = k_S \sin\delta_S$ and $\gamma_S = k_S \cos\delta_S$, from what follows that $\beta^2 = {k_S}^2 - {\gamma_S}^2 = \omega^2/{c_S}^2 - {\gamma_S}^2$.

Likewise the case of an incident P-wave, considering *plane-strain conditions*, $\delta_S = \pi/2$, thus implying that $\gamma_S = 0$ and the shear wavenumber is of the form $\boldsymbol{\beta = k_S = \omega / c_S}$.

5.2. Scattered wave field around a cavity

Considering a circular cylindrical cavity, the incident wave, upon impinging on its contour, will be fully reflected. In accordance with the Huygens' principle [3], after the boundary of the cavity has been struck by the incident wave, each particle on the cavity contour acts as a secondary source generating waves that propagate away from the structure. Thus generated waves constitute the scattered waves. The solution to the diffraction problem, which is based on direct application of the Huygens' theory and satisfies the condition of radiation at infinity, is always unique.

5.2.1. Scattered wave field induced by an incident plane harmonic P-wave

When the incident P-wave arrives at the contour of an empty circular cylindrical cavity, it will be fully returned back into the medium. For the case of an elastic, homogeneous, isotropic medium, two waves are reflected from the boundary – a P-wave with component φ and an S-wave with components ψ and χ. In accordance with the discussion presented in Section 3.2 and the particular solution to the Helmholtz equation in circular coordinates given by Eq. (29), the **scattered waves** are assumed as:

$$\varphi^{scat}(r,\theta,z,t) = \mathrm{e}^{\mathrm{i}(\gamma_p z-\omega t)} \sum_{n=-\infty}^{\infty} A_n(\omega)\, H_n^{(1)}(\alpha r)\, \mathrm{e}^{\mathrm{i}n\theta} \tag{34}$$

$$\psi^{scat}(r,\theta,z,t) = \mathrm{e}^{\mathrm{i}(\gamma_S z-\omega t)} \sum_{n=-\infty}^{\infty} B_n(\omega)\, H_n^{(1)}(\beta r)\, \mathrm{e}^{\mathrm{i}n\theta} \tag{35}$$

$$\chi^{scat}(r,\theta,z,t) = \mathrm{e}^{\mathrm{i}(\gamma_S z-\omega t)} \sum_{n=-\infty}^{\infty} C_n(\omega)\, H_n^{(1)}(\beta r)\, \mathrm{e}^{\mathrm{i}n\theta} \tag{36}$$

where the superscript "*scat*" has the meaning of the scattered field.

The shear wavenumber of the scattered S-waves is related to the compressional wavenumber of the incident P-wave by $\beta^2 = {k_S}^2 - {\gamma_P}^2 = \omega^2/{c_S}^2 - {\gamma_P}^2 = \kappa^2 {k_P}^2 - {\gamma_P}^2 = {k_P}^2(\kappa^2 - \cos^2\delta_P)$, where the coefficient $\kappa = c_P/c_S = k_S/k_P$ as a function of Poisson's ratio ν is:

$$\frac{c_P}{c_S} = \kappa = \sqrt{\frac{\lambda+2\mu}{\mu}} = \sqrt{\frac{2(1-\nu)}{1-2\nu}} \tag{37}$$

Therefore, the **total wave field** then would be:

$$\begin{cases} \varphi = \varphi^{inc} + \varphi^{scat} \\ \psi = \psi^{scat} \\ \chi = \chi^{scat} \end{cases} \tag{38}$$

The unknown scattering coefficients A_n, B_n, and C_n are to be determined for appropriate boundary conditions that must be satisfied on the surface of the body.

The appropriate **boundary condition** for a cylindrical cavity of radius b is a traction-free surface at $r = b$ ($0 \leq \theta \leq 2\pi$), i.e. vanishing radial stress and shear stress components:

$$\begin{cases} \sigma_{rr} = 0 \\ \sigma_{r\theta} = 0 \\ \sigma_{rz} = 0 \end{cases} \qquad r = b \tag{39}$$

The corresponding stresses are in terms of the displacement potentials due to all the waves (see Appendix). The coefficients for each order of n are obtained in the closed form. The stress and displacement fields are determined once the coefficients are known.

5.2.2. Scattered wave field induced by an incident plane harmonic S-wave

The scattering problem considering an incident plane S-wave can be solved in the same manner as the case of a plane P-wave. Namely, **scattered waves** induced by an incident S-wave are also representable by Eqs. (34)–(36), only with the relation of the compressional wavenumber of the scattered P-waves to the shear wavenumber of the incident S-wave given by $\alpha^2 = {k_P}^2 - {\gamma_S}^2 = \omega^2/{c_P}^2 - {\gamma_S}^2 = {k_S}^2/\kappa^2 - {\gamma_P}^2 = {k_S}^2(1/\kappa^2 - \cos^2\delta_S)$.

Considering that $\kappa = c_P/c_S > 1$ (the longitudinal wave velocity c_P is always greater than the transverse wave velocity c_S), the wave number α will be imaginary whenever $\cos\delta_s \geq 1/\kappa^2$. By that, the Hankel function $H_n^{(1)}(i\alpha r)$ changes to the nonoscillatory modified Bessel function of the second kind $K_n(\alpha r)$ [2]. The value $\delta_s = \cos^{-1}(1/\kappa^2)$ represents the critical angle, which is the same as the angle for the case of the total reflection of an SV-wave by a plane surface. For values below the critical angle, the scattered P-wave becomes the surface wave that decays rapidly away from the surface of cylinder.

The **total wave field**, considering the case of an incident plane harmonic S-wave scattered by an empty circular cylindrical cavity embedded in an elastic medium, is:

$$\begin{cases} \varphi = \varphi^{scat} \\ \psi = \psi^{inc} + \psi^{scat} \\ \chi = \chi^{inc} + \chi^{scat} \end{cases} \tag{40}$$

Lastly, it could be concluded that it is easy to calculate displacements and stresses in the medium around a cylindrical cavity as long as the unknown coefficients are determined. Using the boundary conditions on the surface of the cavity (Eq. (39)), along with the condition of radiation at infinity of the secondary wave field scattered by the cavity contour, and with the orthogonality conditions provided by the sinusoidal functions [3], the unknown coefficients could be determined for each order of n.

5.3. Scattered and refracted wave fields for a tunnel

5.3.1. Scattered wave field induced by an incident plane harmonic waves

The analysis of wave motion considering a tunnel of infinite extent with an elastic lining of arbitrary thickness laid in an infinite elastic medium, which is treated as an

elastic hollow circular cylinder, can be carried out in a completely analogous manner. If the elastic constants and the density of the medium λ_{med}, μ_{med}, and ρ_{med} are different from those of the tunnel lining (λ_{lin}, μ_{lin}, and ρ_{lin}), for an incident plane P- or an incident S-wave there are still two reflected waves, as in the previuosly considered case of a cavity, expressed in terms of the corresponding potentials:

$$\varphi^{scat}(r,\theta,z,t) = \mathrm{e}^{\mathrm{i}(\gamma_{p_{med}} z-\omega t)} \sum_{n=-\infty}^{\infty} A_n(\omega)\, H_n^{(1)}(\alpha_{med} r)\, \mathrm{e}^{\mathrm{i}n\theta} \tag{41}$$

$$\psi^{scat}(r,\theta,z,t) = \mathrm{e}^{\mathrm{i}(\gamma_{s_{med}} z-\omega t)} \sum_{n=-\infty}^{\infty} B_n(\omega)\, H_n^{(1)}(\beta_{med} r)\, \mathrm{e}^{\mathrm{i}n\theta} \tag{42}$$

$$\chi^{scat}(r,\theta,z,t) = \mathrm{e}^{\mathrm{i}(\gamma_{s_{med}} z-\omega t)} \sum_{n=-\infty}^{\infty} C_n(\omega)\, H_n^{(1)}(\beta_{med} r)\, \mathrm{e}^{\mathrm{i}n\theta} \tag{43}$$

5.3.2. Refracted wave field in the tunnel lining

If the refracted waves are considered as **propagating waves** [2, 7, 8] there are two refracted waves that propagate outwards from the inner boundary of the liner and two refracted waves that propagate towards the inside of the liner from its outer boundary. Therefore, there will be two inward propagating waves and two outward propagating waves, and then the total displacement potentials in the tunnel lining are:

$$\varphi^{ref}(r,\theta,z,t) = \mathrm{e}^{\mathrm{i}(\gamma_{p_{lin}} z-\omega t)} \sum_{n=-\infty}^{\infty} \left[D_n(\omega)\, H_n^{(1)}(\alpha_{lin} r) + E_n(\omega)\, H_n^{(2)}(\alpha_{lin} r)\right] \mathrm{e}^{\mathrm{i}n\theta} \tag{44}$$

$$\psi^{ref}(r,\theta,z,t) = \mathrm{e}^{\mathrm{i}(\gamma_{s_{lin}} z-\omega t)} \sum_{n=-\infty}^{\infty} \left[F_n(\omega)\, H_n^{(1)}(\beta_{lin} r) + G_n(\omega)\, H_n^{(2)}(\beta_{lin} r)\right] \mathrm{e}^{\mathrm{i}n\theta} \tag{45}$$

$$\chi^{ref}(r,\theta,z,t) = \mathrm{e}^{\mathrm{i}(\gamma_{s_{lin}} z-\omega t)} \sum_{n=-\infty}^{\infty} \left[L_n(\omega)\, H_n^{(1)}(\beta_{lin} r) + M_n(\omega)\, H_n^{(2)}(\beta_{lin} r)\right] \mathrm{e}^{\mathrm{i}n\theta} \tag{46}$$

where the superscript "*ref*" stands for the refracted field. The $H_n^{(1)}$ and $H_n^{(2)}$ terms in the series represent the outward and inward propagating simple harmonic circular waves, respectively.

Alternatively the four refracted waves in the liner might be thought as **standing waves**, that is, the waves being confined in the tunnel lining [3, 9]. In the solutions of the Bessel equations the cylindrical Bessel functions of the second kind have to be retained. Accordingly, the total displacement potentials in the tunnel lining are:

$$\varphi^{ref}(r,\theta,z,t) = \mathrm{e}^{\mathrm{i}(\gamma_{p_{lin}} z-\omega t)} \sum_{n=-\infty}^{\infty} \left[D_n(\omega)\, J_n(\alpha_{lin} r) + E_n(\omega)\, Y_n(\alpha_{lin} r)\right] \mathrm{e}^{\mathrm{i}n\theta} \tag{47}$$

$$\psi^{ref}(r,\theta,z,t) = \mathrm{e}^{\mathrm{i}(\gamma_{s_{lin}} z-\omega t)} \sum_{n=-\infty}^{\infty} \left[F_n(\omega)\, J_n(\beta_{lin} r) + G_n(\omega)\, Y_n(\beta_{lin} r)\right] \mathrm{e}^{\mathrm{i}n\theta} \tag{48}$$

$$\chi^{ref}(r,\theta,z,t) = \mathrm{e}^{\mathrm{i}(\gamma_{s_{lin}} z-\omega t)} \sum_{n=-\infty}^{\infty} [L_n(\omega)\, J_n(\beta_{lin} r) + M_n(\omega)\, Y_n(\beta_{lin} r)]\, \mathrm{e}^{\mathrm{i}n\theta} \quad (49)$$

Both variants have been tried in the study [10]. The trials have revealed that if the refracted waves are represented in terms of propagating waves, a solution will fail in obeying the corresponding boundary conditions at the tunnel–ground interface, in particular for the case of a stiff liner in a soft rock. Moreover, the convergence of the solution based on this representation of refracted seismic waves has not been accomplished with respect to the case of two structures in close proximity. According to these conslusions, in derivation of the solution, the representation of refracted waves in terms of standing waves has been employed. In the author's opinion, this representation is more realistic, since it is rather difficult to trace the refraction of waves across a lining with thickness of finite dimension; so that, transmitted waves are considered to be reflected back and forth between the two surfaces, thus resulting in a standing wave across the tunnel lining cross-section.

5.3.3. Total wave fields in the surrounding medium and the tunnel lining

Considering the medium, the resultant waves are determined by superposing the incident and the reflected waves, whereas the refracted waves are the only ones in the tunnel lining.

Hence, for the case of an *incident P-wave*, the **total wave outside the cylinder** is given by:

$$\begin{cases} \varphi_{med} = \varphi^{inc} + \varphi^{scat} \\ \psi_{med} = \psi^{scat} \\ \chi_{med} = \chi^{scat} \end{cases} \quad (50)$$

whereas for the case of an *incident S-wave*, the total wave field in the surrounding medium is:

$$\begin{cases} \varphi_{med} = \varphi^{scat} \\ \psi_{med} = \psi^{inc} + \psi^{scat} \\ \chi_{med} = \chi^{inc} + \chi^{scat} \end{cases} \quad (51)$$

On the other hand, the **total wave field inside the tunnel lining**, both for the case of *an incident P-wave* and the case of *an incident S-wave*, will be:

$$\begin{cases} \varphi_{lin} = \varphi^{ref} \\ \psi_{lin} = \psi^{ref} \\ \chi_{lin} = \chi^{ref} \end{cases} \quad (52)$$

5.3.4. Boundary conditions

Considering the case of a tunnel structure, the resulting nine sets of unknown expansion coefficients in the above presented equations are comprised of three for the reflected waves and six for the refracted waves. To solve for these unknowns,

corresponding boundary conditions in terms of six equations at the outer radius $r = b$ and three equations at the inner radius $r = a$ should be used.

Most of analytical and numerical models are based on the assumption that the contact between the lining and the surrounding medium is of perfect nature. Accordingly, the **no-slip boundary conditions** at the lining–ground adjoining surface ($r = b$, $0 \leq \theta \leq 2\pi$) are continuity of the radial and the shear stresses and displacements across the interface for reasons of equilibrium:

$$\begin{cases} \sigma_{rr,med} = \sigma_{rr,lin} & u_{r,med} = u_{r,lin} \\ \sigma_{r\theta,med} = \sigma_{r\theta,lin} & u_{\theta,med} = u_{\theta,lin} \\ \sigma_{rz,med} = \sigma_{rz,lin} & u_{z,med} = u_{z,lin} \end{cases} \qquad r = b \tag{53}$$

Considering the inner lining surface ($r = a$, $0 \leq \theta \leq 2\pi$), **stress-free boundary conditions** should be prescribed:

$$\begin{cases} \sigma_{rr,lin} = 0 \\ \sigma_{r\theta,lin} = 0 \\ \sigma_{rz,lin} = 0 \end{cases} \qquad r = a \tag{54}$$

In many elastodynamic problems, however, the bond between the liner and the surrounding ground may be imperfect [11, 12].

The spring model is one of the popular models for describing a wide range of contacts between the liner and surrounding ground, from perfect contact to disconnected media [8, 9]. Using this concept, the general boundary conditions to be applied at the interface of the elastic tunnel lining and the surrounding medium are:

$$\begin{cases} \sigma_{rr,med} = \sigma_{rr,lin} & \sigma_{rr,med} = k_r(u_{r,med} - u_{r,lin}) \\ \sigma_{r\theta,med} = \sigma_{r\theta,lin} & \sigma_{rr,med} = k_\theta(u_{\theta,med} - u_{\theta,lin}) \\ \sigma_{rz,med} = \sigma_{rz,lin} & \sigma_{rz,med} = k_z(u_{z,med} - u_{z,lin}) \end{cases} \tag{55}$$

where k_r, k_θ, and k_z are radial, transverse, and axial stiffness (bonding) parameters per unit length, respectively.

The values of these parameters are infinity, with the normal, tangential, and axial stresses being finite quantities, for the case of *perfectly bonded interface* (i.e., *no-slip contact*), in which case the normal, tangential, and axial stresses and displacements are continuous at the interface. When $k_r \to \infty$, $k_z \to \infty$, and $k_\theta \to 0$, which implies that $\sigma_{r\theta} = 0$, the *full-slip condition* (i.e., *perfect slip with no friction*) in *r*-θ (transverse) direction has been defined. The intermediate values of these parameters correspond to the *imperfect contact* (i.e., *loose contact*) in the given direction. In the case when all of the stiffness parameters tend to 0, and therefore, $\sigma_{rr} \to 0$, $\sigma_{r\theta} \to 0$, and $\sigma_{zz} \to 0$, implying that no waves are transmitted from the surrounding medium to the tunnel lining, the case equivalent to the case of a tunnel without liner (cavity) applies.

Based on Eqs. (50)–(52), consequently, the stresses in the medium will depend on incident and scattered wave potentials, whereas the stresses in the cylinder are contributed by refracted waves only.

Using the equations for the stresses and displacements (see Appendix), with the proper cylindrical functions, the unknown scattering and transmission coefficients can be determined by simultaneous algebraic equations.

6. Translational Addition Theorems for Cylindrical Wave Functions

In many difrraction and scattering problems, waves of one characteristic shape (coordinate system) that are incident upon a boundary of some other shape (coordinate system) need to be considered. In such cases, it is difficult to satisfy boundary conditions on that surface. Namely, Bessel functions are not algebraic functions, and they are not simply periodic functions, and particularly, that they are not doubly periodic functions. Consequently, it is not possible to express $J_n(kr_i + kr_j)$ as an algebraic function of $J_n(kr_i)$ and $J_n(kr_j)$. That is to say, that Bessel functions do not possess addition theorems in the strict sense of the term [5].

Nevertheless, a class of mathematical relationships called *wave transformations* (*translational addition theorems for bi-cylindrical coordinates*) exists, which overcomes this difficulty in many cases by allowing the fields scattered by the various interfaces to be studied, all referred to a common origin.

Fig. 9 illustrates two systems of Cartesian rectangular coordinates O_1, x_1, y_1 and O_2, x_2, y_2 with identically oriented and parallel respective axes, and the polar coordinate systems r_1, θ_1 and r_2, θ_2 related to them by the corresponding conversion formulas. The point P of the plane xOy is an arbitrary point.

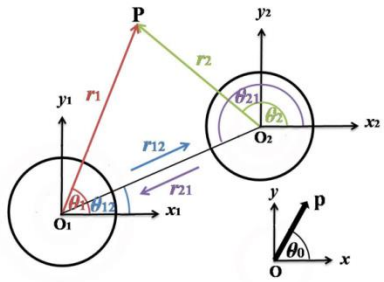

Fig. 9 Addition theorem for cylindrical wave function (reproduced after [6]).

The addition theorems are of the following form [6]:

$$J_n(kr_i)\,\mathrm{e}^{\mathrm{i}n\theta_i} = \sum_{m=-\infty}^{\infty} J_{n-m}(kd)\,J_m\left(kr_j\right)\,\mathrm{e}^{\mathrm{i}(n-m)\theta_{ij}+\mathrm{i}m\theta_j} \qquad d \gtrless r_j \qquad (56)$$

$$H_n^{(1),(2)}(kr_i)\,\mathrm{e}^{\mathrm{i}n\theta_i} = \sum_{m=-\infty}^{\infty} H_{n-m}^{(1),(2)}(kd)\,J_m\left(kr_j\right)\,\mathrm{e}^{\mathrm{i}(n-m)\theta_{ij}+\mathrm{i}m\theta_j} \qquad d > r_j \qquad (57)$$

$$H_n^{(1),(2)}(kr_i)\,\mathrm{e}^{\mathrm{i}n\theta_i} = \sum_{m=-\infty}^{\infty} H_{n-m}^{(1),(2)}\left(kr_j\right)\,J_m(kd)\,\mathrm{e}^{\mathrm{i}(n-m)\theta_j+\mathrm{i}m\theta_{ij}} \qquad d < r_j \qquad (58)$$

in which θ_{ij} ($i, j = 1, 2, i \neq j$) is angle between the OjOi line and the x_i-axis, and d is the distance between two neighbouring structures.

With the above relationships between d and r_j, all the presented expansions converge absolutely and uniformly.

Formulae in Eqs. (56)–(58) allow each Bessel or Hankel wave function written in an i-th system of coordinates ($i = 1$ or $i = 2$) to be expressed through the same wave functions, but written in another, the j-th system of coordinates ($j \neq i$; $j = 2$ or $j = 1$).

These formulas play a significant role in the problems of scattering of waves on several circular cylinders. By using them, the dynamic interaction between closely spaced structures is fully taken into consideration. The appropriate relationship to be used, in order to determine unknown scattering coefficients, would be the equation for which the condition that the bodies are not tangent to one another is satisfied (i.e., $r_i < d$).

7. SUMMARY AND CONCLUDING REMARKS

Tunnels are crucial facilities in transportation network, and occurrence of a seismic event can cause a loss of human lives and damage to the infrastructures. It could severely influence the rescue and repair work after earthquake directly due to intermission of the transportation network and affect the economy of a region due to the time required to restore the functionality of the network. In addition, there is a lack of systematic and precisely established seismic design rules for tunnels that are of great importance [13]. Particularly the case of closely running tunnel structures should be turned into an important direction of further development of seismic design codes, where the aspect of their minimum seismically safe distance should be an issue of all concerns [10].

If it is possible to establish a realistic constitutive model for material behaviour, identify the boundary conditions, and combine these with the equations of equilibrium and compatibility, an exact theoretical solution on the seismic response of tunnel structures can be obtained. A closed-form solution is the ultimate method of analysis, in which all solution requirements are satisfied and the theories of mathematics are used to obtain complete analytical expressions defining the full behaviour of the problem.

The mathematical tool, presented in this work, completes the necessary background required for the exact analysis of the problem of seismic wave scattering and refraction on a circular cylindrical cavity or tunnel of infinite length, or the problem accompanying two closely located circular cylinders, embedded in a homogeneous, elastic, isotropic medium of infinite extent. Essential advantage of the exact analytical solution is in terms of better accuracy, thus offering the best benchmark for comparison with other solutions obtained by more conventional simplified asymptotic approaches or numerical methods.

APPENDIX

A.1. Displacement components in terms of displacement potentials

$$u_r = \frac{\partial \varphi}{\partial r} + \frac{1}{r}\frac{\partial \psi}{\partial \theta} + \frac{\partial^2 \chi}{\partial r\, \partial z} \tag{A.1}$$

$$u_\theta = \frac{1}{r}\frac{\partial \varphi}{\partial \theta} - \frac{\partial \psi}{\partial r} + \frac{1}{r}\frac{\partial^2 \chi}{\partial \theta\, \partial z} \tag{A.2}$$

$$u_z = \frac{\partial \varphi}{\partial z} + \left(\frac{\partial^2 \chi}{\partial z^2} - \nabla^2 \chi\right) \tag{A.3}$$

A.2. Stress components in terms of displacement potentials

$$\sigma_{rr} = \lambda\left(\frac{\partial u_r}{\partial r} + \frac{u_r}{r} + \frac{1}{r}\frac{\partial u_\theta}{\partial \theta} + \frac{\partial u_z}{\partial z}\right) + 2\mu\frac{\partial u_r}{\partial r} =$$

$$= \lambda\nabla^2\varphi + 2\mu\left[\frac{\partial^2 \varphi}{\partial r^2} + \frac{\partial}{\partial r}\left(\frac{1}{r}\frac{\partial \psi}{\partial \theta}\right) + \frac{\partial^3 \chi}{\partial r^2\, \partial z}\right] \tag{A.4}$$

$$\sigma_{\theta\theta} = \lambda\left(\frac{\partial u_r}{\partial r} + \frac{u_r}{r} + \frac{1}{r}\frac{\partial u_\theta}{\partial \theta} + \frac{\partial u_z}{\partial z}\right) + 2\mu\left(\frac{u_r}{r} + \frac{1}{r}\frac{\partial u_\theta}{\partial \theta}\right) =$$

$$= \lambda\nabla^2\varphi + 2\mu\left[\frac{1}{r}\left(\frac{\partial \varphi}{\partial r} + \frac{1}{r}\frac{\partial^2 \varphi}{\partial \theta^2}\right) + \frac{1}{r}\left(\frac{1}{r}\frac{\partial \psi}{\partial \theta} - \frac{\partial^2 \psi}{\partial r\, \partial \theta}\right) + \frac{1}{r}\left(\frac{\partial^2 \chi}{\partial r\, \partial z} + \frac{1}{r}\frac{\partial^3 \chi}{\partial \theta^2\, \partial z}\right)\right] \tag{A.5}$$

$$\sigma_{zz} = \lambda\left(\frac{\partial u_r}{\partial r} + \frac{u_r}{r} + \frac{1}{r}\frac{\partial u_\theta}{\partial \theta} + \frac{\partial u_z}{\partial z}\right) + 2\mu\frac{\partial u_z}{\partial z} =$$

$$= \lambda\nabla^2\varphi + 2\mu\left\{\frac{\partial^2 \varphi}{\partial z^2} + \left[\frac{\partial^3 \chi}{\partial z^3} - \frac{\partial}{\partial z}(\nabla^2 \chi)\right]\right\} \tag{A.6}$$

$$\sigma_{r\theta} = \mu\left(\frac{1}{r}\frac{\partial u_r}{\partial \theta} + \frac{\partial u_\theta}{\partial r} - \frac{u_\theta}{r}\right) =$$

$$= \mu\left\{2\left[\frac{1}{r}\frac{\partial^2 \varphi}{\partial r\, \partial \theta} - \frac{1}{r^2}\frac{\partial \varphi}{\partial \theta}\right] + \left[\frac{1}{r^2}\frac{\partial^2 \psi}{\partial \theta^2} - r\frac{\partial}{\partial r}\left(\frac{1}{r}\frac{\partial \psi}{\partial r}\right)\right] + 2\left[\frac{1}{r}\frac{\partial^3 \chi}{\partial r\, \partial \theta\, \partial z} - \frac{1}{r^2}\frac{\partial^2 \chi}{\partial \theta\, \partial z}\right]\right\} \tag{A.7}$$

$$\sigma_{rz} = \mu\left(\frac{\partial u_r}{\partial z} + \frac{\partial u_z}{\partial r}\right) =$$

$$= \mu\left\{2\frac{\partial^2 \varphi}{\partial r\, \partial z} + \frac{1}{r}\frac{\partial^2 \psi}{\partial \theta\, \partial z} + \left[2\frac{\partial^3 \chi}{\partial r\, \partial z^2} - \frac{\partial}{\partial r}(\nabla^2 \chi)\right]\right\} \tag{A.8}$$

$$\sigma_{\theta z} = \mu\left(\frac{\partial u_\theta}{\partial z} + \frac{1}{r}\frac{\partial u_z}{\partial \theta}\right) =$$

$$= \mu\left\{\frac{2}{r}\frac{\partial^2 \varphi}{\partial \theta\, \partial z} - \frac{\partial^2 \psi}{\partial r\, \partial z} + \left[\frac{2}{r}\frac{\partial^3 \chi}{\partial \theta\, \partial z^2} - \frac{1}{r}\frac{\partial}{\partial \theta}(\nabla^2 \chi)\right]\right\} \tag{A.9}$$

Acknowledgement. *The authors gratefully acknowledge the support of the "SEEFORM PhD Programme", financed by the German Academic Exchange Service (DAAD). The support of the Ministry of Education, Science, and Technological Development of the Republic of Serbia in the frame of the scientific–research project TR36028 (2011–2020) is also greatly appreciated.*

REFERENCES

1. V. Šešov and K. Talaganov, Soil and Foundation Dynamics – Dynamic Response of Soil, 25th International eleven-week course on aseismic design and construction "CADAC 2006", Institute of Earthquake Engineering and Engineering Seismology (IZIIS), Skopje, 2006.
2. C. C. Mow and H. Y. Pao, The Diffraction of Elastic Waves and Dynamic Stress Concentrations, Report No. R-482-PR, Rand, Santa Monica, California, 1971.
3. J. D. Achenbach, Wave Propagation in Elastic Solids, North Holland Publishing Company – Amsterdam · London, American Elsevier Publishing Company, Inc., New York, 1973.
4. M. Abramowitz and I. A. Stegun, Handbook of Mathematical Functions, United States Department of Commerce, National Bureau of Standards, 1964.
5. G. N. Watson, A Treatise of the Theory of Bessel Functions, Cambridge University Press, London and New York, 1966.
6. Ye. A. Ivanov, Diffraction of Electromagnetic Waves on Two Bodies, National Aeronautics and Space Administration, Washington, DC, 1970.
7. X.-L. Zhou, J.-H. Wang and L.-F. Jiang, "Dynamic response of a pair of elliptic tunnels embedded in a poroelastic medium", Journal of Sound and Vibration 325, 2009, pp. 816-834, doi:10.1016/j.jsv.2009.04.001.
8. C. Yi, P. Zhang, D. Johansson and U. Nyberg, "Dynamic response of a circular lined tunnel with an imperfect interface subjected to cylindrical P-waves", Computers and Geotechnics 55, 2014, pp. 165-171, doi:10.1016/j.compgeo.2013.08.009.
9. S. M. Hasheminejad and R. Avazmohammadi, "Dynamic stress concentrations in lined twin tunnels within fluid-saturated soil", Journal of Engineering Mechanics 134(7), 2008, pp. 542-554, doi**:**10.1061/(ASCE)0733-9399(2008)134:7(542).
10. E. Zlatanović, Contribution to the methods of seismic analysis of twin-tunnel structures, PhD Dissertation, Institute of Earthquake Engineering and Engineering Seismology (IZIIS) of Skopje, University "Ss. Cyril and Methodius" of Skopje, Skopje, Republic of North Macedonia, 2016.
11. E. Zlatanović, G. Broćeta and N. Popović-Miletić, "Numerical modelling in seismic analysis of tunnels regarding soil–structure interaction", Facta Universitatis, Series: Architecture and Civil Engineering 11(3), 2013, pp. 251-267, doi:10.2298/FUACE1303251Z.
12. E. Zlatanović, D. Lukić and V. Šešov, "Presentation of analytical solutions for seismically induced tunnel lining forces accounting for soil–structure interaction effects", Building Materials and Structures 57(1), 2014, pp. 3-28, doi:10.5937/grmk1401003Z.
13. E. Zlatanović, V. Šešov, D. Lukić, Z. Bonić and N. Davidović, "State-of-the-art of seismic design codes for tunnels and underground structures", Scientific Journal of Civil Engineering 8(2), 2019, pp. 49-54.

MATEMATIČKA INTERPRETACIJA RASIPANJA I REFRAKCIJE SEIZMIČKIH TALASA U PRISUSTVU TUNELSKIH OBJEKATA KRUŽNOG POPREČNOG PRESEKA

U fokusu ovog rada je interpretacija difrakcije i rasipanja seizmičkih talasa u polarno-cilindričnim koordinatama primenom odgovarajućeg matematičkog aparata. U radu je najpre dat pregled nekih od najznačajnijih svojstava cilindričnih Bessel-ovih funkcija, koje su podesne za matematičko opisivanje problema difrakcije i rasipanja seizmičkih talasa. Takođe, dat je prikaz jednačina koje predstavljaju osnovu tzv. metode ekspanzije talasnih funkcija (wave function expansion), u polarno-cilindričnim koordinatama i za slučaj seizmičkih talasa sa ravnim frontom. Prikazana su i rešenja primenom metode ekspanzije talasnih funkcija za slučaj nepodgrađenog tunelskog otvora i slučaj podgrađenog tunelskog objekta, sa aspekta fenomena rasipanja i refrakcije seizmičkih talasa, pod uticajem incidentnih harmonijskih P-talasa i S-talasa sa ravnim frontom. Na kraju rada prezentovane su i teoreme translatornog sabiranja (translational addition theorems), koje imaju važnu ulogu u matematičkom rešavanju problema difrakcije i rasipanja seizmičkih talasa u prisustvu dva blisko položena tunelska objekta.

Ključne reči: *kružni tunel, seizmički talasi, rasipanje, refrakcija, Fourier–Bessel-ovi redovi*